Spontaneous Axisymmetry Breaking of Saturn's External Magnetic Field

Peter Goldreich

Institute for Advanced Study, Princeton, New Jersey, USA; pmg@ias.edu

Alison J. Farmer

Department of Astronomy, Harvard University, MS-51, 60 Garden St., Cambridge, Massachusetts, USA; afarmer@cfa.harvard.edu

Received _____; accepted _____

ABSTRACT

Saturn's magnetic field is remarkably axisymmetric. Its dipole axis is inclined by less than 0.2° with respect to its rotation axis. Early evidence for nonaxisymmetry came from the periodicity of Saturn's kilometric radio bursts (SKR). Subsequently, percent variations of the SKR period were found to occur on timescales of years. A recent breakthrough has been the direct detection of a nonaxisymmetric component of the field that rotates with a period close to that of the SKR. Because this component's magnitude varies only weakly with distance from Saturn, it must be supported by currents external to the planet. These currents flow along field lines that connect plasma in the equatorial region of the outer magnetosphere (the plasma disk) to the high latitude ionosphere. The plasma originates from mass lost by the planet's rings and moons. It is tightly coupled to the magnetic field and its motion can be ascribed to the large scale interchange of flux tubes. Heavily loaded tubes drift outward and are replaced by lightly loaded ones which drift inward. *This process of rotationally driven convection is responsible for breaking the axisymmetry of Saturn's external magnetic field.* The convection pattern rotates rigidly with the angular velocity of the plasma at its source. Its rotation provides the clock that controls the periods of both the SKR bursts and the nonaxisymmetric magnetic perturbations. We distinguish two types of currents. Those that flow in the azimuthal direction in both the ionosphere and the plasma disk provide a radial force that enables the plasma to corotate with the planet's spin. They are responsible for stretching magnetic field lines and thus exposing the polar ionosphere to the incoming solar wind. Other currents flow in the latitudinal direction in the ionosphere and the radial direction in the plasma disk. These act to transfer angular momentum from the planet's spin to the outflowing plasma. They slow down the rotation

rate of the ionosphere below that of the underlying atmosphere and are the reason the clock referred to above runs slow. Moreover, these currents are the source of nonaxisymmetric magnetic perturbations whose strength varies inversely with radial distance in the planet's equatorial plane. Quantitative agreement with the magnitude of these perturbations requires a mass loss rate of order $10^4\,\mathrm{g\,s^{-1}}$, similar to that believed to come from Saturn's E-ring.

1. Introduction

Saturn's atmosphere exhibits strong ($\lesssim 400\,\mathrm{m\,s^{-1}}$) and stable (over decadal time scales) zonal winds. This precludes assigning a unique rotation period to its outer layers. Although the planet is fluid throughout, its deep interior must be in near solid body rotation (Liu et al. 2006). Thus the internal rotation rate might be revealed by observing the nonaxisymmetric components of the planet's magnetic field.[1] However, application of this technique to Saturn has been hampered by the extreme axisymmetry of the planet's magnetic field.

Voyager observations of Saturn Kilometric Radiation (SKR) bursts coming from the planet's auroral regions showed a periodicity of 10h 39 min 24 ± 7 s (Desch and Kaiser 1981). The periodicity was suspected to arise from a small non-axisymmetry of the planet's internally generated magnetic field. Detections of small in situ magnetic anomalies from *Voyager* and *Pioneer 11* magnetometers were also reported (Giampieri and Dougherty 2004), with periods consistent with that of the SKR. *Ulysses* observations of the variability of the SKR period, by of order 1 % on timescales of 1 year from 1994 to 1997 (Galopeau

[1]This technique applied to Jupiter has found a rotation period constant to within seconds over 50 years.

and Lecacheux 2000), challenged its interpretation as the rotation period of the planet's deep interior.[2] *Cassini* confirmed this variability, measuring an SKR period of 10h 45min 45 ±45s on approach to Saturn in 2004 (Gurnett et al. 2005). Most recently, magnetometer data obtained by *Cassini* showed a small (∼ few nT) signal with period 10h 47min 6 ±40 s (Giampieri et al. 2006) that was stable during 14 months of observation. Giampieri et al. (2006) suggested that this period might be that of Saturn's interior spin. However, the decline of the perturbation amplitude with radius is too slow to be due to a current source within Saturn, so this interpretation cannot be correct. Instead, we propose that the non-axisymmetric component of Saturn's external magnetic field is generated by rotationally driven convection in the planet's magnetosphere. The convection transports plasma from the inner magnetosphere to the magnetopause where it joins the solar wind. The plan of the paper is as follows. In §2 we provide a simplified version of equations governing rotationally driven magnetospheric convection. We apply these equations in §3 to estimate the nonaxisymmetric magnetic perturbations it produces. §4 is devoted to a discussion of the clock that controls the perturbations' rotation rate. A short summary is given in §5.

1.1. Nominal parameters

We adopt cgs units for length, mass, time, and Gaussian units for electrodynamical quanitites. In order to focus our discussion on Saturn, we provide numerical estimates along with some of the major equations. The parameters used in these evaluations are displayed in Table 1.

[2]A change of 1 % in spin period of the planet's core over such a short timescale is energetically impossible.

Quantity	Value adopted	Notes
R	6×10^9 cm	
Ω	1.6×10^{-4} s^{-1}	
B_P	0.2 G	
Σ_p	$10^{13}\ \Sigma_{p,13}$ cm s^{-1}	[1]
a_i	$4R\ a_{i,4R}$	[2]
$\Delta\phi_i$	$\pi\ \Delta\phi_{i,\pi}$	
$\dot{M}$	$10^4\ \dot{M}_4$ g s^{-1}	[3]
μ	3×10^{-24} g	
γ	1.4	
T	$140\ T_{140}$ K	[4]
ν	$10^8\ \nu_8$ cm^2 s^{-1}	[5]
ρ^I	$3 \times 10^{-13}\ \rho^I_{-12.5}$ g cm^{-3}	[6]
g	1×10^3 cm s^{-2}	

Table 1: The numerical quantities adopted in order of magnitude calculations throughout the paper. The meanings of the symbols are given in the text where first used. Key to numbered notes: [1] scaled between estimates for low and high latitude ionosphere (Atreya et al. 1974); [2] scaled to orbit of E-ring; [3] scaled to estimates for plasma production from Saturn's E-ring (Leisner et al. 2006); [4] scaled to atmospheric temperature at base of ionosphere (Atreya et al. 1974); [5] scaled to eddy diffusion coefficient at homopause (Atreya et al. 1974); [6] scaled between estimates for low latitude ionosphere and auroral ionosphere (Atreya et al. 1974).

2. Basic Electrodynamics

2.1. Rotationally driven magnetospheric convection

The topic has an extensive history, but this is not the place to review it. Instead, we point to a few influential papers that aided our understanding. We have done nothing more than to apply what we learned from reading the literature.

Equations governing rotationally driven convection were formulated by Chen (1977) and by Hill et al. (1981). Many applications have been made to the outward transport of mass from the Io plasma torus. Pontius and Hill (1989) includes a clear discussion of different approaches to this problem.

Progress in solving the equations referred to above has been slow. In retrospect, this is not surprising. They are nonlinear set, which probably precludes finding analytic solutions. Moreover, realistic applications are faced with including a continuous supply of plasma along with boundary conditions that simulate its loss to the solar wind at the magnetopause.

Perhaps the most ambitious attempt at a realistic solution is that by Yang et al. (1994) who applied the Rice convection model to the Io torus. They investigated an initial value problem, the instability of a torus of finite width. An active source of plasma was not included. Long fingers were found to grow radially outward from the torus. This is not surprising. The initial state is analogous to that of a heavier fluid resting on top of a lighter one which is Rayleigh-Taylor unstable. But unlike the standard Rayleigh-Taylor instability which takes place for constant gravitational acceleration, the instability of the plasma torus is driven by centrifugal acceleration which increases linearly outward. This increase allows narrow fingers to run away from the more slowly developing, thicker modes that might otherwise subsume them.

In the absence of anything better, we adopt a simplified picture of steady-state magnetospheric convection. A tongue of plasma flows outward from a torus of neutral material that is escaping from Enceladus. Plasma is continuously created inside the torus by ionization of this material. It exits in a tongue which flows outward. Except within the tongue, flux tubes outside the torus drift inward due to "fringing" electric fields surrounding the tongue region. As they cross the torus, the inward-moving tubes are loaded with freshly created plasma. Then their trajectories bend around so that they join the back of the tongue. In this manner, plasma is continuously removed from the entire torus even though the tongue emanates from only a limited range of azimuth.

In order for the convection pattern to remain steady, plasma must consistently outflow from the same range of azimuth in the rotating frame. Outflow occurs from the densest part of the torus, and so if a single tongue is to carry the outgoing material, its base must always be refilled fast enough so that no other longitudes in the torus can accumulate more plasma. Inwardly drifting tubes, which empty the rest of the torus of plasma, drift more slowly than those moving outwards, because the electric fields in the inward-drifing tubes cannot be larger than the internal tongue fields which they "fringe". Only if the base of the tongue spans $\Delta\phi_i \gtrsim \pi$ radians can the inwards drift velocity be large enough to keep the plasma content in the rest of the torus lower than in the tongue region.

We have been able to bolster this description with simplified models of electrostatic fields, but much remains to be done before anything rigorous might emerge. A serious technical issue is that a smooth tongue of plasma is likely to develop narrower fingers as discussed above. Fortunately, the conclusions of our investigation are insensitive to this possibility. However, it would certainly impede a rigorous calculation of the convection pattern. That will have to be left for the future.

2.2. Notation

We adopt spherical polar coordinates r, θ, ϕ and work in the inertial frame. Saturn's magnetic field is approximated as a spin aligned dipole. The ionosphere is taken to rotate with uniform angular velocity Ω.[3] Where necessary, superscripts ^{M} and ^{I} are used to distinguish magnetospheric and ionospheric quantities, and ^{Ip} to denote the direct (Pedersen) component of the ionospheric current. B_r and B_θ are the components of the unperturbed magnetic field at a general field point. R is Saturn's radius and a is the orbital radius in the equatorial plane. B_P is the magnetic field intensity on the equator in Saturn's ionosphere and B_z is the component of the *vertical* magnetic field in the magnetic equator at a;

$$B_z = -\left(\frac{R}{a}\right)^3 B_P \,. \tag{1}$$

Height integrated current densities and electrical conductivities are indicated by J and Σ, respectively. The surface mass density in the magnetosphere is denoted by σ.

2.3. Dipole magnetic fields

Components of a spin aligned dipole magnetic field take the form

$$B_r = \frac{2M\cos\theta}{r^3} \qquad B_\theta = \frac{M\sin\theta}{r^3}\,, \tag{2}$$

where M is the dipole moment. The field magnitude is

$$B = \left(B_r^2 + B_\theta^2\right)^{1/2} = \frac{M}{r^3}(1+3\cos^2\theta)^{1/2}\,. \tag{3}$$

A individual field line is labeled by either the colatitude of its footprint at $r = R$, denoted by θ_0, or by its maximum radial extent a; $a\sin^2\theta_0 = R$. Its shape is described by:

$$r\sin^2\theta_0 = R\sin^2\theta \qquad \text{or} \qquad r = a\sin^2\theta\,. \tag{4}$$

[3]Except in §4 where Ω denotes the angular velocity of the deep atmosphere.

We are interested in field lines that connect to the planet at high latitudes. Thus we simplify our expressions by setting $\sin\theta_0 = (R/a)^{1/2}$ and $\cos\theta_0 = 1$.

2.4. Magnetospheric currents

Consider an element of cold plasma that is nearly corotating with and slowly drifing away from the planet. Centrifugal balance and angular momentum conservation require that the height integrated current densities which pass through the element satisfy[4]

$$\frac{J_\phi^M B_z}{c} = -\sigma\Omega^2 a \tag{5}$$

and

$$\frac{J_a^M B_z}{c} = -2\sigma\Omega\dot{a} \tag{6}$$

respectively.

The ratio

$$\frac{J_a^M}{J_\phi^M} = \frac{2\dot{a}}{\Omega a} \tag{7}$$

is small in the inner magnetosphere but becomes of order unity in its outer regions.

2.5. Ionospheric direct currents

The horizontal divergence of the magnetospheric currents, $\nabla_{2\mathrm{d}} \cdot \mathbf{J}^M$, flows along magnetic field lines and closes in the ionosphere. This determines the components of the direct (Pedersen) current in the ionosphere. They read

$$J_\phi^{Ip} = \frac{1}{R}\frac{da}{d\theta_0}\frac{J_\phi^M}{2} = -\frac{c\sigma\Omega^2 R}{B_P}\left(\frac{a}{R}\right)^{11/2} , \tag{8}$$

[4]We neglect the planet's gravity in equation (5)

and

$$J_\theta^{Ip} = \frac{a}{R\sin\theta_0}\frac{J_a^M}{2} = \frac{c\sigma\Omega R}{B_P}\left(\frac{a}{R}\right)^{11/2}\frac{\dot{a}}{a}\,. \tag{9}$$

Their ratio is given by

$$\frac{J_\theta^{Ip}}{J_\phi^{Ip}} = -\frac{\dot{a}}{\Omega a}\,. \tag{10}$$

The ionospheric Hall current, $\mathbf{J}^{Ih}$, is not fixed in this manner. Because its horizontal divergence vanishes,[5] its determination requires knowledge of the ionospheric electric field.

2.6. Ionospheric electric field

The height-integrated current density, $\mathbf{J}^I$, and electric field, $\mathbf{E}^I$, are related by[6]

$$\mathbf{J}^I = \mathbf{J}^{Ip} + \mathbf{J}^{Ih} = \Sigma_p\mathbf{F}^I + \Sigma_h(\hat{\mathbf{b}}\times\mathbf{E}^I)\,, \tag{11}$$

where $\mathbf{F}^I \equiv \mathbf{E}^I + (\mathbf{\Omega}\times\mathbf{R})\times\mathbf{B}^I/c$ is the Lorentz force, Σ_p and Σ_h are the height-integrated Pederson and Hall conductivities, and $\mathbf{b} \equiv \mathbf{B}^I/|\mathbf{B}^I|$. Taking the divergence of equation (11) yields

$$\nabla_{2d}\cdot\mathbf{J}^I = \nabla_{2d}\cdot\mathbf{J}^{Ip} = \Sigma_p\nabla_{2d}\cdot\mathbf{E}^I\,. \tag{12}$$

$\nabla_{2d}\cdot\mathbf{J}^{Ih} = 0$ because $\nabla_{2d}\times\mathbf{E}^I = 0$; $\mathbf{E}^I$ is a potential field. A full solution for $\mathbf{E}^I$ would involve setting $\mathbf{E} = -\nabla\Phi^I$ and then solving Poisson's equation $\nabla^2\Phi^I = -\Sigma_p\nabla_{2d}\cdot\mathbf{J}^{Ip}$. As detailed in §2.1, for realistic conditions, this has proven to be a difficult task. Fortunately, a simpler procedure suffices for the purposes of the current investigation.

We set

$$F_\theta = \frac{J_\theta^{Ip}}{\Sigma_p} \qquad \text{and} \qquad E_\phi = \frac{J_\phi^{Ip}}{\Sigma_p}\,, \tag{13}$$

[5]Provided the Hall conductivity is independent of position as we assume it to be.

[6]By setting $\sin\theta_0 = (R/a)^{1/2}$ and $\cos\theta_0 = 1$, we neglect both B_θ^I and the effects of the parallel conductivity.

with

$$F_\theta \equiv E_\theta - \frac{2\Omega R \sin\theta}{c} B_P \,. \tag{14}$$

This procedure does a good job evaluating $\mathbf{E}^I$ in the portion of the ionosphere that is magnetically connected to the outgoing tongue of magnetospheric plasma. However, it does not permit a determination of the fields that fringe this region. These control the inward flow of depleted plasma tubes.

2.7. E×B drift

Just above the ionosphere, the plasma drifts at velocity

$$\mathbf{v} = c\left(\frac{E_\phi}{2B_P}\hat{\mathbf{e}}_\theta - \frac{E_\theta}{2B_P}\hat{\mathbf{e}}_\phi\right) \,. \tag{15}$$

Projecting down to the magnetosphere, we obtain

$$\frac{\dot{a}}{a} = -\frac{2\dot{\theta}_0}{\theta_0} = -\frac{cE_\phi}{RB_P}\left(\frac{a}{R}\right)^{1/2} = \frac{c^2\sigma\Omega^2}{\Sigma_p B_P^2}\left(\frac{a}{R}\right)^6 \,. \tag{16}$$

and

$$\frac{\Delta\Omega}{\Omega} = \frac{cF_\theta}{2\Omega R B_P}\left(\frac{a}{R}\right)^{1/2} = \frac{c^2\sigma}{2\Sigma_p B_P^2}\left(\frac{a}{R}\right)^6 \frac{\dot{a}}{a} \,. \tag{17}$$

Here $\Delta\Omega$ is the angular velocity at which the plasma in the tongue slips relative to the rotation at the top of the ionosphere.

For future reference, we note that

$$\left(\frac{\dot{a}}{a}\right)^2 = 2\Omega\Delta\Omega \,. \tag{18}$$

2.8. Coupling to rate of mass loss

Suppose the tongue covers $\Delta\phi(a)$ in azimuth where $\Delta\phi$ is a function of a to be determined later. Then

$$\dot{M} = \Delta\phi a \dot{a} \sigma \,. \tag{19}$$

Substituting for $\dot{a}$ using equation (16), we arrive at

$$\dot{M} = \frac{\Delta\phi c^2 \sigma^2 \Omega^2 R^2}{\Sigma_p B_P^2} \left(\frac{a}{R}\right)^8 , \tag{20}$$

from which we obtain

$$\sigma = \frac{|B_P|}{c\Omega R} \left(\frac{\Sigma_p \dot{M}}{\Delta\phi}\right)^{1/2} \left(\frac{R}{a}\right)^4 . \tag{21}$$

Next we replace σ in $\dot{a}/a$ which yields

$$\frac{\dot{a}}{a} = \frac{\Omega c}{R|B_P|} \left(\frac{\dot{M}}{\Sigma_p \Delta\phi}\right)^{1/2} \left(\frac{a}{R}\right)^2 . \tag{22}$$

2.9. Steady-state scalings

Flux freezing implies that σ/B_z is independent of a in a sourceless, steady-state flow. Consequently, $\Delta\phi$ at a is related to its initial value at a_i by

$$\Delta\phi = \left(\frac{a_i}{a}\right)^2 \Delta\phi_i \,. \tag{23}$$

Thus

$$\sigma = \frac{|B_P|}{c\Omega a_i} \left(\frac{\Sigma_p \dot{M}}{\Delta\phi_i}\right)^{1/2} \left(\frac{R}{a}\right)^3 . \tag{24}$$

$$\dot{a} = \frac{R\Omega c}{a_i |B_P|} \left(\frac{\dot{M}}{\Sigma_p \Delta\phi_i}\right)^{1/2} \left(\frac{a}{R}\right)^4 . \tag{25}$$

Somewhat arbitrarily, we adopt a_o, the value of a where $\dot{a} = \Omega a$, or equivalently where $\Delta\Omega = -\Omega/2$, as the outer radius of the region in which partial corotation applies;

$$\left(\frac{a_o}{R}\right) = \left(\frac{a_i |B_P|}{c}\right)^{1/3} \left(\frac{\Sigma_p \Delta\phi_i}{\dot{M}}\right)^{1/6} \sim 21 \left(\frac{a_{i,4R}^2 \Delta\phi_{i,\pi} \Sigma_{p,13}}{\dot{M}_4}\right)^{1/6} . \tag{26}$$

The timescale $a/\dot{a}$ for outward plasma transport decreases with distance from the planet. Plasma near the source at a_i doubles its radial distance in a time ~ 10 days. The constancy of the observed magnetic period on far longer timescales implies that the convection pattern remains steady for many dynamical timescales of the source region.

3. Magnetic Perturbations

3.1. Opening of the polar cusp

The azimuthal current J_ϕ^M creates a radial component of magnetic field just above and below the tongue of outgoing plasma;

$$\Delta B_r = \frac{2\pi J_\phi^M}{c} \mathrm{sgn}(z)\,. \tag{27}$$

Applying equations (24) and (26), we find that these field lines bulge outward relative to vertical by an angle

$$\tan\alpha = \frac{|\Delta B_r|}{B_z} = \frac{2\pi\sigma\Omega^2 a}{B_z^2} = \frac{2\pi\Omega a_o \Sigma_p}{c^2}\left(\frac{a}{a_o}\right)^4 \sim 1.4\left(\frac{a_{i,4R}^2 \Delta\phi_{i,\pi}\Sigma_{p,13}^7}{\dot{M}_4}\right)^{1/6}. \tag{28}$$

The stretching of these field lines is a consequence of the centripetal acceleration they impart to the plasma.

If α attains a substantial value at a_o, the exposure of Saturn's polar cap to the incoming solar wind will be enhanced along the range of longitudes subtended by the outer parts of the tongue.[7] This could account for the preferential emission of the SKR within a narrow range of longitudes.

---

[7]The field lines bulge only above and below the outgoing plasma. Because $\Delta\phi \propto a^{-2}$, $\Delta\phi_0$ may be quite small, even if $\Delta\phi_i$ is of order π.

3.2. Magnetic anomalies measurable by spacecraft

The radial current in the tongue of outgoing material at a is given by

$$I_a^M = a\Delta\phi J_a^M = -\frac{2c\Omega\dot{M}}{B_z}\,. \tag{29}$$

Thus

$$\frac{dI_a^M}{da}da = -\frac{6c\Omega\dot{M}}{aB_z}da \tag{30}$$

is the current that flows along the strip of field lines connecting the ionosphere (in each hemisphere) to the tongue between a and $a + da$. It is notable that I_a^M depends on the rate of mass loss but not on the pattern of outflow.

To estimate the magnetic perturbation produced by this current, we approximate it as flowing along a thin wire of infinite extent which passes the observation point at distance s. Then

$$\frac{d\delta B}{da} \approx \frac{2}{cs}\frac{dI_a^M}{da} \approx \frac{12\Omega\dot{M}}{RB_P s}\left(\frac{a}{R}\right)^2\,. \tag{31}$$

We focus on perturbations in the equatorial region of the inner magnetosphere, since this is where the *Cassini* magnetometer has found evidence for non-axisymmetric field components. For an observer in the equatorial plane at radius ϖ, the minimum distance s between the observer and a "wire" of dipole field-aligned current which passes through the equator at $a \gg \varpi$ is $s \simeq \varpi$. Substituting for s in Eq. 31 and integrating to a_o, we find

$$\delta B \approx \frac{4\Omega\dot{M}}{B_P\varpi}\left(\frac{a_o}{R}\right)^3 \approx \frac{4\,a_i\Omega}{c\varpi}\left(\Sigma_p\dot{M}\Delta\phi_i\right)^{1/2} \sim 1.2\times10^{-5}\ \mathrm{G}\ (\Delta\phi_{i,\pi}\dot{M}_4\Sigma_{p,13})^{1/2}\,. \tag{32}$$

The above estimate for the magnitude of the magnetic perturbations ignores the contribution from the return current that comes from $a > a_o$ and closes the circuit. Unfortunately, not much can be deduced about the geometry of the return current since the field lines it flows along are likely to be strongly perturbed by the solar wind. However, it is possible that it could act to reduce the perturbation magnitude, perhaps by a factor 2.

We have also ignored the contribution from the currents that flow in the opposite (N versus S) hemisphere. In the case of perfect N-S symmetry, magnetic perturbations from the two hemispheres would exactly cancel in the middle of the tongue but not elsewhere. In reality, at most times [8] this cancelation is likely to be small, since the ionospheric conductivity will differ in the northern and southern polar ionospheres. Near solstice, almost all the current will flow through the summer hemisphere. At these times the estimate for δB should be doubled.

As illustrated in Figure 1, the field-aligned (Birkeland) currents supplying J_ϕ^M to the tongue occur in closely spaced, oppositely directed pairs. The magnetic perturbations produced by these "line dipoles" are small at distances large compared to their spacing. Thus, although they are typically smaller, the field-aligned currents feeding J_a^M dominate the magnetic perturbations present in the magnetosphere.

The fragmentation of the plasma tongue into narrower structures would have a minor effect on the magnetic perturbations produced by the currents supplying J_a^M, but would further weaken those produced by the currents supplying J_ϕ^M.

Analysis of the variation of the measured components of δB with position in the magnetosphere would test our model.

4. The Clock

As described in §1, a somewhat slow and imperfect clock controls the quasi-periodic behavior of SKR bursts. In our scenario the same clock controls the magnetic anomalies. Both *Voyager*- and *Cassini*-era measurements of SKR and magnetic periods are consistent

[8] The exception being near times of equinox.

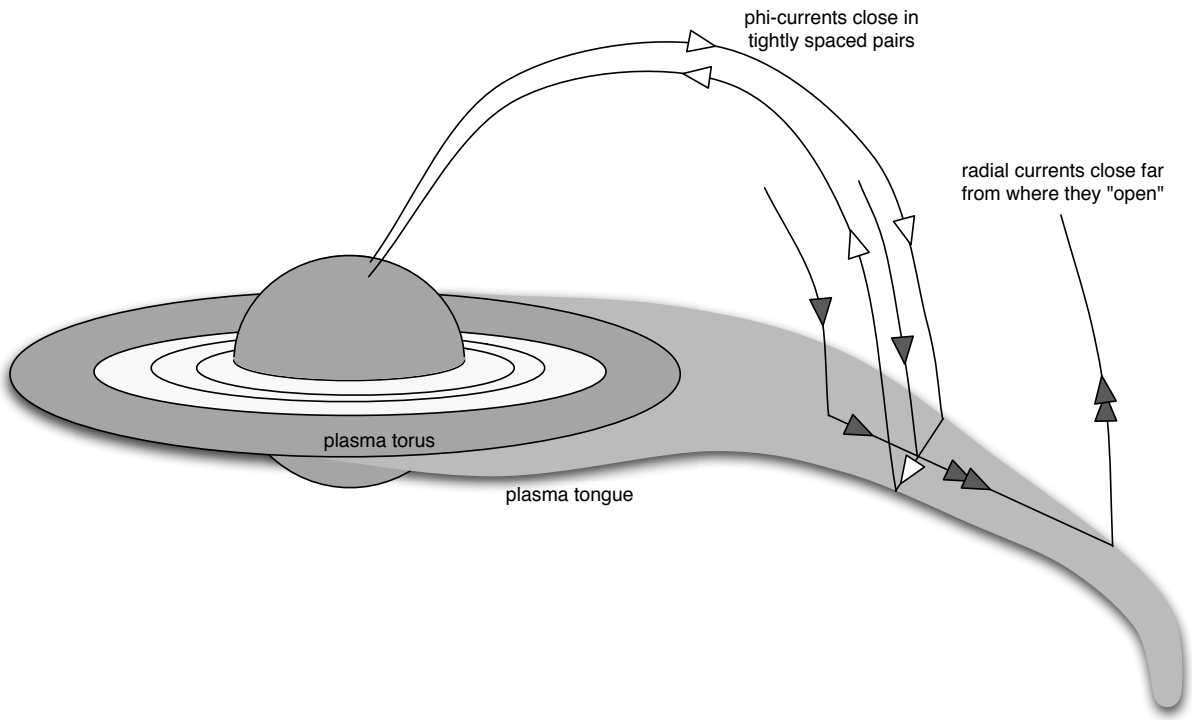

Fig. 1.— The currents associated with the plasma tongue in Saturn's magnetosphere: azimuthal currents occur in close opposite pairs, and so their contribution to magnetic perturbations is small.

with this picture.

4.1. Where is the clock located?

The clock is located in the inner magnetosphere and beats at the period of rotation of the asymmetry associated with the inner portion of the plasma outflow.[9] As explained below, the clock's period propagates throughout the magnetosphere provided the differential

[9]Our working hypothesis is that the E-ring centered at $a \approx 4R$ around the orbit of Enceladus is the dominant plasma source.

rotation of the latter remains time invariant.

Suppose that a source of material located at radius a_i feeds a plasma torus rotating at Ω_i. The torus is unstable and sends out a "tongue" of plasma centered on a fixed azimuth $\phi_c(a_i)$ in the rotating frame. Plasma at the center of the tongue moves outwards at radial speed $\dot{a}_c(a)$, and orbits at angular speed $\dot{\phi}_c(a)$, where $\dot{\phi}_c(a) \lesssim \Omega_i$. In steady-state, the shape of the tongue's centerline would be determined by

$$\phi_c(a) = \phi_c(z_i) + \int_{a_i}^{a} da' \, \frac{\dot{\phi}_c(a')}{\dot{a}_c(a')} \, . \tag{33}$$

Viewed from a nonrotating frame, the tongue is a steady structure rotating at pattern speed Ω_i. At radius a and time t, the apparent azimuth of the tongue's centerline is given by

$$\phi_{\rm obs} = \phi_c(a) + \Omega_i t, \tag{34}$$

and so $\dot{\phi}_{\rm obs} = \Omega_i$, regardless of the run of differential rotation across the magnetosphere.

4.2. Why is the clock slow?

SKR and magnetic periods determined by Cassini are longer than those associated with the motion of any atmospheric features. The most plausible explanation is that the ionosphere rotates more slowly than the atmosphere below it because magnetic torques are transferring angular momentum from it to the plasma tongue.[10]

Since the magnetic torque increases sharply with increasing latitude, this is also a plausible explanation for the observed decline of the magnetosphere's angular velocity with

[10]Huang and Hill. (1989) concluded that the rotation of Jupiter's ionosphere is slowed in this manner.

increasing distance from Saturn. We shall show that this scenario is qualitatively reasonable, in contrast to models based on the slippage of the rotation of the magnetospheric plasma relative to the rotation of the ionosphere. Most of the way out, the plasma maintains good corotation with the part of the ionosphere to which it is connected, but the ionosphere is subcorotating with respect to the underlying atmosphere. The observed clock frequency is the rotation rate of the ionosphere where it connects to the inner part of the plasma tongue.

4.2.1. Steady-state rotation of the ionosphere

We analyze a simple model for the steady-state rotation of the ionosphere and underlying atmosphere. It assumes axial symmetry and considers only vertical transport of angular momentum. Deep atmospheric layers are taken to rotate rigidly with angular velocity Ω. We work within the approximation of an isothermal atmosphere with sound speed c_s, scale height $H = c_s^2/\gamma g$, buoyancy frequency $N^2 = (\gamma - 1)g/(\gamma H)$, and eddy diffusivity ν. The ionosphere is taken to be a single layer rotating at the angular velocity Ω^M of the part of the plasma tongue to which it is magnetically connected.

We modify equation (6) to allow for the nonuniform rotation rate, Ω^M, of the magnetospheric plasma. The torque per unit a applied to the tongue of outgoing plasma reads

$$\frac{dT_B^M}{da} = \dot{M}\frac{d}{da}\left(\Omega^M a^2\right) . \tag{35}$$

Thus the magnetic torque per unit θ_0 on the northern ionosphere is given by

$$\frac{dT_B^I}{d\theta_0} = \frac{\dot{M}R^2}{2}\frac{d}{d\theta_0}\left(\frac{\Omega^M}{\theta_0^4}\right) . \tag{36}$$

In steady state, the torque must be constant with depth below the ionosphere. Provided the torque is not too large, a stable, steady-state, shear flow is established in which the

viscous torque given by

$$\frac{dT_\nu}{d\theta_0} = -2\pi R^4 \theta_0^3 \rho\nu \frac{d\Omega^A}{dz}\,, \tag{37}$$

carries angular momentum up from the atmosphere to the ionosphere. Equating the viscous torque to the magnetic torque yields

$$\frac{d\Omega^A}{dz} = \frac{\dot{M}}{4\pi R^2 \rho\nu\theta_0^3} \frac{d}{d\theta_0}\left(\frac{\Omega^M}{\theta_0^4}\right)\,. \tag{38}$$

The shear flow is stable where the Richardson criterion is satisfied, that is where equation (38) predicts

$$R\theta_0 \frac{d\Omega}{dz} \lesssim N\,. \tag{39}$$

In the stable regime,

$$\Omega - \Omega^M \approx -\frac{\dot{M}H}{4\pi R^2 \rho^I \nu\theta_0^3} \frac{d}{d\theta_0}\left(\frac{\Omega^M}{\theta_0^4}\right) \approx \frac{\dot{M}\Omega H}{\pi R^2 \rho^I \nu\theta_0^8}\,. \tag{40}$$

Here we have set $\Omega^M = \Omega$ in the final step. This is a good approximation since $\Omega - \Omega^M \ll \Omega$ in the stable regime.

The boundary of the stable regime occurs where the stability criterion is violated just below the ionosphere. We use the symbol Θ_0 to denote the value of θ_0 at this boundary. At Θ_0,

$$\frac{\dot{M}}{4\pi R \rho^I \nu N \Theta_0^2} \frac{d}{d\theta_0}\left(\frac{\Omega^M}{\theta_0^4}\right) \approx -1\,. \tag{41}$$

An approximate solution for Θ_0, and the corresponding $a_{\rm crit}/R \equiv \Theta_0^{-2}$, follows from setting $\Omega^M = \Omega$: In this manner we arrive at

$$\frac{a_{\rm crit}}{R} = \left(\frac{1}{\Theta_0^2}\right) \approx \left(\frac{\pi R \rho^I \nu N}{\dot{M}\Omega}\right)^{2/7} \sim 9.1 \left(\frac{\nu_8 \rho^I_{-12.5}}{\dot{M}_4 T_{140}^{1/2}}\right)^{2/7}\,. \tag{42}$$

The unstable layer penetrates deeper into the atmosphere poleward of Θ_0. Because the angular velocity gradient in the stable layer is inversely proportional to density, and the density increases exponentially with depth, the thickness of the unstable layer increases

logarithmically with decreasing θ_0. An estimate for $\Omega - \Omega^M$ is obtained by multiplying the critical angular velocity gradient from equation (39) by the thickness of the unstable layer. The following expression provides a good fit to $\Omega - \Omega^M$ for all values of θ_0 or a/R. We express it in terms of the latter for ease of comparison with data on the rotation of plasma in Saturn's magnetosphere.

$$1 - \frac{\Omega^M}{\Omega} \approx \frac{NH}{\Omega R}\left(\frac{a}{R}\right)^{1/2} \ln\left[1 + \left(\frac{a}{a_{\rm crit}}\right)^{7/2}\left(\frac{\Omega^M}{\Omega} + \frac{a}{2\Omega}\frac{d\Omega^M}{da}\right)\right] . \tag{43}$$

Figure 2 displays the run of $v_\phi = \Omega^M a$ vs a/R for our nominal parameters. The rotation curve is in reasonable agreement with *Voyager* measurements (Richardson 1986). At $a/R = 4$, corresponding to the orbit of Enceladus and the brightest portion of the E-ring, $1 - \Omega^M/\Omega \simeq 0.5\%$. By comparison, equation (18) predicts the much smaller value, 3×10^{-5}, for the slippage of the rotation rate in the plasma tongue at $a = 4R$ relative to that of the ionosphere.

4.3. Why Is the Clock Imperfect?

The ionospheric rotation rate responds to changes in a variety of parameters, including the atmosphere's eddy diffusion coefficient, the ionosphere's height-integrated conductivity, and the rate of mass loss from the magnetosphere. All of these are likely to have a seasonal dependence. Solar weather, including short term variations in the solar wind ram pressure and longer term variations over the solar activity cycle also affect the conductivity in the auroral ionosphere.

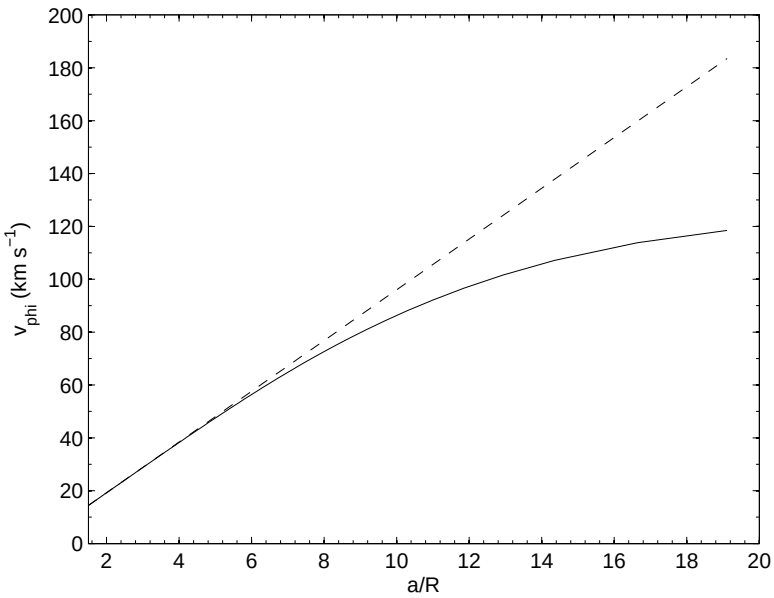

Fig. 2.— Orbital velocity of equatorial plasma as a function of distance from Saturn. Rigid corotation with Saturn's interior is plotted as the dashed line; the magnetosphere lags the planetary interior due to slowing of the ionosphere by magnetic torques.

5. Summary

Rotationally driven convection of magnetospheric plasma breaks the axisymmetry of Saturn's external magnetic field. Field aligned currents transfer angular momentum from the planet to a tongue of outflowing plasma. This transfer slows the rate of rotation of the ionosphere relative to that of the underlying atmosphere. The currents are the source for the non-axisymmetric components of the field. The common rotation rates of these components and Saturn's kilometric radio (SKR) bursts is that of the plasma near the orbit of Enceladus, and by extension the rotation rate in the ionosphere to which this plasma is coupled. This rate tells us nothing about the rotation rate of Saturn's deep interior. Of that we remain ignorant.

Magnetic perturbations with magnitudes similar to those observed by *Cassini* are produced for $\dot{M} \approx 10^4$ g s^{-1}, a value similar to estimates for the rate of production of plasma from Saturn's E-ring.

Enhancement of the SKR occurs in a narrow range of longitudes where the tip of the outgoing plasma stream connects to the auroral ionosphere via field lines that are bowed outwards by currents that supply the plasma's centripetal acceleration.

REFERENCES

Atreya, S. K., Donahue, T. M., Nagy, A. F., Waite, Jr., J. H., McConnell, J. C. 1984. Theory, measurements, and models of the upper atmosphere and ionosphere of Saturn. IN Saturn (A85-33976 15-91), Tucson, AZ, University of Arizona Press, 239-277.

Chen, C.-K. 1977. Topics in planetary plasmaspheres. Ph.D. thesis, UCLA.

Desch, M. D., Kaiser, M. L. 1981. Voyager measurement of the rotation period of Saturn's magnetic field. Geophysical Research Letters 8, 253-256.

Galopeau, P. H. M., Lecacheux, A. 2000. Variations of Saturn's radio rotation period measured at kilometer wavelengths. Journal of Geophysical Research 105, 13089-13102.

Giampieri, G., Dougherty, M. K. 2004. Rotation rate of Saturn's interior from magnetic field observations. Geophysical Research Letters 31, 16701.

Giampieri, G., Dougherty, M. K., Smith, E. J., Russell, C. T. 2006. A regular period for Saturn's magnetic field that may track its internal rotation. Nature 441, 62-64.

Gurnett, D. A., and 26 colleagues. 2005. Radio and Plasma Wave Observations at Saturn from Cassini's Approach and First Orbit. Science 307, 1255-1259.

Hill, T. W., Dessler, A. J., Maher, L. J. 1981. Corotating magnetospheric convection. Journal of Geophysical Research 86, 9020-9028.

Huang, T. S. and Hill, T. W. 1989. Corotation lag of the Jovian atmosphere, ionosphere, and magnetosphere. Journal of Geophysical Research 94, 3761-3765.

Leisner, J. S., Russell, C. T., Dougherty, M. K., Blanco-Cano, X., Strangeway, R. J., Bertucci, C. 2006. Ion cyclotron waves in Saturn's E ring: Initial Cassini observations. Geophysical Research Letters 33, 11101.

Liu, J.J., Goldreich, P., Stevenson, D. Ohmic Dissipation Constraint on Deep-seated Zonal Winds on Jupiter and Saturn. Icarus submitted.

Pontius, Jr., D. H. and Hill, T. W. 1989. Rotation driven plasma transport - The coupling of macroscopic motion and microdiffusion. Journal of Geophysical Research 94, 15041-15053.

Richardson, J. D. 1986. Thermal ions at Saturn - Plasma parameters and implications. Journal of Geophysical Research 91, 1381-1389.

Yang, Y. S., Wolf, R. A., Spiro, R. W., Hill, T. W. and Dessler, A. J. 1994. Journal of Geophysical Research 99, 8755-8770.